Chemistry-Inspired Charge-Pump Frequency Synthesiser

1st Massimo Monti
Elettronica Monti
Ponte a Egola, Italy
Email: massimo@elettronicamonti.it

2nd Elena Puri
Elettronica Monti
Ponte a Egola, Italy
Email: elena@elettronicamonti.it

3rd Mario Monti
Elettronica Monti
Ponte a Egola, Italy
Email: monti@elettronicamonti.it

***Abstract*—Phase-Locked Loops (PLLs) are frequently used for frequency synthesis. The working principle consists in minimising the phase difference between a reference frequency and the synthesised tone. A periodic pulse, with a relatively high constant frequency and a modulated width, pulls up or down a Charge Pump that adjusts the voltage at the input of a Voltage Control Oscillator and thus compensates the phase difference. In this paper we propose a novel, Chemistry-inspired approach that reviews the working principle of traditional PLLs: the charge pump is corrected with constant-width pulses that are scheduled with a rate that is a function of the frequency error. Such an approach brings two main benefits. First, comparison spurs do not appear as the correction happens with long time intervals and thus spurs are buried in the output tone. Second, there is no theoretical limitation in the resolution of the output frequency, and de facto, Chemistry-inspired frequency synthesisers have the same advantage of fractional PLLs in terms of frequency resolution but have no drawbacks in terms of RF spectral purity.**

***Index Terms*—Chemistry-inspired algorithms, fractional spurs, frequency synthesis, PFD spurs, PLL.**

I. Introduction

Charge Pump Phase Locked Loops (CP-PLLs) are widely used in communication systems and measuring apparatus for clock generation and frequency synthesis. In a PLL, a Phase and Frequency Detector (PFD) detects the phase error between output and reference tones. This error modulates the width of periodic pulses that drive a Charge Pump (CP). The CP output provides the correction signal that, through the Loop Filter (LF), is then applied to a Voltage Control Oscillator (VCO) in order to compensate the detected phase difference [1]. CP-PLL circuit performs frequency synthesis based upon the PFD comparison frequency, f_{PFD}. In integer PLLs, the output frequency is an integer multiplier of the PFD frequency and thus, the frequency resolution is very limited. To improve the frequency resolution, in fractional PLLs, an additional modulator circuitry changes dynamically and in the right proportion the modulus of the frequency divider and produces an output frequency that is a fraction of f_{PFD}.

The presence of periodic (T_{PFD}) pulses that adjust the VCO input translates in spurious tones in the output spectrum. Indeed, nonidealities of PFD and CP[1] make it necessary to converge a certain amount of energy at f_{PFD}. If in integer PLLs spurs exhibit fairly low levels, in fractional PLLs, where the modulator introduces phase errors in every reference cycle by varying the frequency divider modulus, spurs exhibit significant levels and multiple intermodulated tones appear in the output spectrum. Moreover, several factors like capacitive leakage, or metal parasitics increase the magnitude of PFD spurs in fractional PLLs [2]. Many works have focused on the reduction of PFD spurs studying CP current mismatch, for example by reducing the reverse leakage current at the CP [3] or by amplitude-controlling the current mismatch at the CP [4]. Other works focused instead on reducing leakage currents at the LF, for example by estimating the leakage currents based on pulse width difference [5], or by compensation of the digitally calibrated leakage current at the LF during a limited calibration period [6]. Another line of research (e.g., [7],[8]) is exploring all-digital PLLs where the adoption of a Digital-to-Time Converter (DTC) and a digitally controlled VCO eliminates analog circuitries and the related issues.

In this paper, we propose a Chemistry-inspired CP frequency synthesiser. We approach frequency synthesis from a new perspective: The train of pulses that are applied to the LF have a constant width but an error-modulated rate. This has the advantage to spread the energy for adjusting the VCO input around values that are orders lower than the output frequency.

The Chemistry-inspired CP frequency synthesiser can be represented by the block diagram in Fig. 1, which is very similar to that of a classic PLL. A Chemistry-inspired Algorithm (CA) controls the CP module. In general terms, CAs represent a class of algorithms whose logic is described as a chemical reaction network. Inputs, outputs and internal states are represented by concentrations of molecular species, and their (mathematical) relationships are represented by reaction rules. CAs are subject to chemical kinetics (e.g. the Law of Mass Action - LoMA), which dominate operations and influence the behavioural characteristics of the algorithm, and make it intrinsically *robust* and *analysable* [9],[10],[11].

[1]Examples of nonidealities are *(i)* CP current mismatch, *(ii)* reset delay (dead zone) of the PFD, *(iii)* propagation delay mismatch between the up and down paths from the PFD to the CP and *(iv)* flow of leakage currents through the CP switches to the LF due to charge injection and clock feedthrough [2].

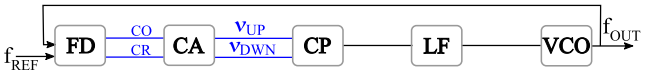

Figure 1. Block diagram of a Chemistry-inspired frequency synthesiser. The Chemical Algorithm (CA) modulates the rate of constant-width pulses at the CP input.

In practice, the reference counter (CR) and the output frequency counter (CO), out of the Frequency Detector (FD) module, represent the integer inputs of the CA module, which is programmed with the chemical reaction set formally shown in Fig. 2. The output reactions trigger constant-width CP pulses with rates v_{UP} that pump the VCO up and v_{DWN} that pump it down. The synthesiser output frequency is tuned by programming the divider N related to CO. In theory, there is no limitation in the frequency resolution (limitations arise from implementation details such as resolution in frequency detection). At the same time, the output spectrum does not exhibit drawbacks in terms of spurs.

The remainder of this paper is organised as follows. In Sect. II, we formally define a CA and clarify the laws that govern its dynamics. In Sect. III, we describe the HW implementation and report on Lab experiment results. In Sect. IV, we discuss features of the CA-controlled CP frequency synthesiser. Finally, we conclude in Sect. V.

II. Chemistry-Inspired Algorithms (CAs).

The logic of CAs is expressed with a network diagram of chemical reactions among molecular species (e.g., Fig. 2) rather than, as for traditional algorithms, with state diagrams and pseudocode. The species represent the algorithm's inputs, outputs, and internal state variables. Reactions capture the causal relationships between the system's state-variables.

Formally, a CA is represented by a set $\mathcal{S}$ of molecular species, and a set $\mathcal{R}$ of reaction rules of the general form

$$r \in \mathcal{R}: \quad \sum_{s\in\mathcal{S}} \alpha_{r,s} s \xrightarrow{k_r} \sum_{s\in\mathcal{S}} \beta_{r,s} s \tag{1}$$

where, k_r is the *reaction coefficient* (a constant), $\alpha_{r,s}$ is the *stoichiometric reactant coefficient* and $\beta_{r,s}$ is the *stoichiometric product coefficient*. Specifically, reaction r replaces $\alpha_{r,s}$ amount of molecules from each species $s \in \mathcal{S}$ with $\beta_{r,s}$ amount of molecules of each species $s \in \mathcal{S}$ at an average rate controlled by the k_r-coefficient. *I.e.*, the formal description of the reaction set drawn in Fig. 2 is reported below as a set of reaction equations (details on CA reaction equations in [11]).

$$\begin{aligned}
r_1&: \ \text{EM} \xrightarrow{k_{\text{in}}} \text{EM}+\text{ED} & r_2&: \ 2\text{EM} \longrightarrow \text{EM}\\
r_3&: \ \text{EM}+\text{CR} \longrightarrow 2\text{EM}+\text{CR} & r_4&: \ \text{CR}+\text{EP} \longrightarrow \text{CR}\\
r_5&: \ \text{EP}+\text{CO} \longrightarrow 2\text{EP}+\text{CO} & r_6&: \ \text{CO}+\text{EM} \longrightarrow \text{CO}\\
r_7&: \ \text{EP} \xrightarrow{k_{\text{in}}} \text{EP}+\text{EU} & r_8&: \ 2\text{EP} \longrightarrow \text{EP}\\
r_9&: \ \text{ED} \xrightarrow{k_{\text{out}}} +\emptyset & r_{10}&: \ \text{EU} \xrightarrow{k_{\text{out}}} +\emptyset
\end{aligned}$$

E.g., reaction r_3 consumes, if present, one molecule of species EM and one of species CR and produces 2 molecules of species EM and one molecule of species CR.

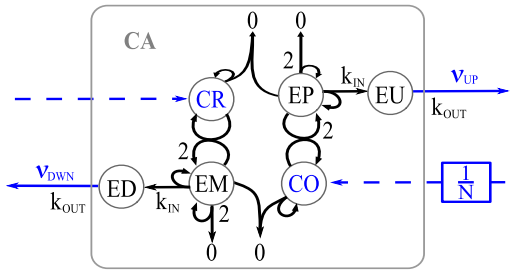

Figure 2. Reaction diagram for the CA-controlled frequency synthesiser. Molecular species CO and CR are the CA inputs and reflect the current state of counters related to the actual output frequency (CO) and the reference frequency (CR). N is the divider of CO counter. Rates v_{UP} and v_{DWN} represent the CA outputs, namely rates of Up-Charge-Pump 10ns-pulses (v_{UP}) and Down-Charge-Pump 10ns-pulses (v_{DWN}). Species EP and EM reflect respectively the positive and negative error, merely controller's state variables.

Dynamics of CAs (when and which reaction is executed) are regulated by the LoMA, which states that the average rate $v_r(t)$ of occurrence of a chemical reaction $r \in \mathcal{R}$ is proportional to its reactant concentrations [11]:

$$v_r(t) = k_r \prod_{s\in\mathcal{S}} c_s^{\alpha_{r,s}}(t) \tag{2}$$

where $c_s(t)$ is the amount of molecules of species $s \in \mathcal{S}$ at time t and k_r is the reaction speed coefficient.

The LoMA couples the state and the dynamics of the system, and plays a key role in CAs (as a self-adaptive internal scheduler). For example, in the CA-controlled frequency synthesiser in Fig. 2, the effectiveness of the controller stems from the strict relation that the LoMA imposes between the current state of the system (frequency error) and the rates v_{UP} and v_{DWN} of output reactions that drive the CP up and down, respectively. The smaller the frequency error, the lower the adjusting rate. By comparison, in PLLs, the phase difference between reference and output tones is adjusted periodically at a constant rate (phase difference modulates the pulse width).

The behaviour of CAs is mathematically expressed as a fluid model which can be directly derived from (1), in the form of a set of Ordinary Differential Equations (ODEs):

$$\dot{\mathbf{c}}(t) = \boldsymbol{\Xi} \cdot \mathbf{v}(\mathbf{k}, \mathbf{c}(t)) \tag{3}$$

where $\boldsymbol{\Xi}$ is the matrix made of stoichiometric reactant coefficients $\alpha_{r,s}$. By studying (3) at steady states it follows that

$$v_{\text{UP}} = k_{\text{in}} \cdot (c^*_{\text{CO}} - c^*_{\text{CR}}) \qquad (c^*_{\text{CO}} > c^*_{\text{CR}}) \tag{4a}$$

$$v_{\text{DWN}} = k_{\text{in}} \cdot (c^*_{\text{CR}} - c^*_{\text{CO}}) \qquad (c^*_{\text{CR}} > c^*_{\text{CO}}) \tag{4b}$$

where v_{DWN} is the rate of pull-down triggering reaction r_9, and v_{UP} that of pull-up triggering reaction r_{10}. Thus, the CA-controlled frequency synthesiser in Fig. 2 produces a (constant-width) pulse on the pull-down output with a rate proportional to the difference between reference and output frequency counter (when the reference counter is higher than the output one), and, vice-versa, it produces a (constant-width) pulse on the pull-up output with a rate proportional to the difference between output and reference frequency counters (when the output counter is higher than the reference one).

III. Implementation and Experimental Results

We have developed a board where a classic CP-PLL and the novel CA-controlled CP frequency synthesiser coexist. Specifically, the board has an RF switch (ADG709) to change at run time the CP input of TI-LMX2592 PLL, a commercial PLL performant in terms of RF spectral purity. The customised LF can be bypassed so that the CA of Fig. 2 can drive the CP directly (thus the VCO). The implementation of the CA module consists mainly in two fundamental blocks. *(i)* In an FPGA (XC6SLX9), the two counters related to the reference input and the output frequency are updated at high speed (2 GHz). These counters represent species CR and CO respectively. *(ii)* In a microcontroller (TI-MSP430F5659), the chemical reaction depicted in Fig. 2 is implemented, and the output reactions with rates v_{UP} and v_{DWN} trigger a 10ns-width pulse on the pull-up and pull-down branches of the CP. Reaction coefficients were set to 1000 (see theory in [11]). The reference frequency of 47,169811 MHz was generated with EM-AT10 RF generator that provided an extremely frequency-stable and spurious-free output tone. We selected 47.169811 MHz as a reference frequency because this value[2] is not a multiple of the system clock value (10 MHz) and we wanted that possible related spurs were well distinguishable as they were not related to phenomena under study. As we set the PLL divider to 8 (to synthesise 3.75 GHz), the PFD frequency was 5.89622 MHz.

For the first test we measured the output spectrum when LMX2592 PLL was programmed in order to work in integer mode (best RF purity) and generated a tone at 3.75 GHz. Results are shown in Fig. 3, where the output tone is visible in the centre of the spectrum. As from the theoretical prediction obtained with simulator PLLATINUMSIM-SW (we do not show simulation results for the sake of space), two PFD spurs are visible at ± 5.89 MHz away from the output frequency with levels around -90 dBc. This result is directly comparable with the spectrum in Fig. 4 that was obtained with the CA-controlled CP frequency synthesiser when the reference was programmed to 3.75 GHz; no PFD spurs are visible.

For the second test, we programmed LMX2592 PLL to work in fractional mode, with two different values for the numerator. Thanks to the fractional operating mode, the output frequency could be tuned with steps of 122.838 kHz (denominator set to 96). We first set the PLL numerator to 3, see blue curve in Fig. 5; fractional spurs appear at ± 0.184 MHz away from the output tone with the highest level (≈31 dBc), and at multiple frequencies with lower levels, as expected from theory. Then, we set the PLL numerator to 4, see magenta curve in Fig. 5. Also in this case, fractional spurs appear; highest levels show up at ± 0.346 MHz away from the output tone (with levels ≈36 dBc), and at multiple frequencies with lower levels (as from theoretical predictions).

We programmed the CA to synthesise similar tones, first at 3.7503685 GHz, see blue curve in Fig. 6, and then at 3.7504914 GHz, see magenta curve in Fig. 6. No spurs are visible. Also in broadband, spurs do not show up (experiments not reported for space limitations).

[2]The frequency of 47.169811 MHz is one of the fixed values that can be generated with EM AT10 RF generator.

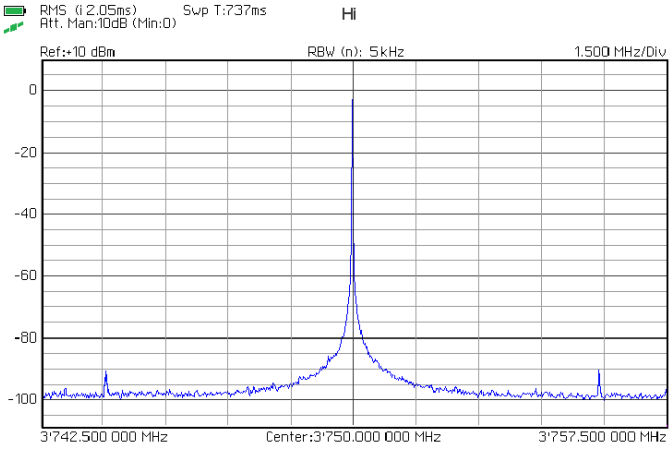

Figure 3. Locked PLL LMX9522 used in Integer mode with PFD=5.89622 MHz. Reference spurs at ± 5.89 MHz are detectable.

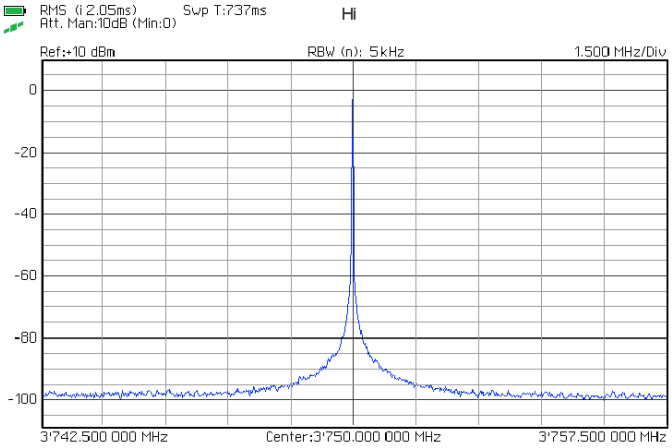

Figure 4. CA-controlled LMX9522; reference programmed to 3.75 GHz.

IV. Discussion

Nonidealities caused by real-world analog circuitry, such as CP leakage currents or voltage disturbances in VCO, do characterise Chemistry-inspired synthesisers too. However, these nonidealities are not compensated by converging the energy at the PFD frequency, which has a high value in order to guarantee good performance and thus creates spurs that are close to the output frequency. On the contrary, thanks to the way the CA schedules CP pulses, the energy spreads around the steady-state reaction rate, which is orders lower than the output frequency. In the experiments, the reaction that triggered CP pull-up pulses had a rate of roughly 28 Hz.

In the experimental tests, the output of the CA-controlled frequency synthesiser exhibits the same phase noise as that of the classic PLL (≈105 dBc/Hz@100 kHz). However, low-frequency jitter may appear if the system does not have a sufficient granularity: in our implementation, the width of CP driving pulses was 10 ns (limitation coming from the specifica-

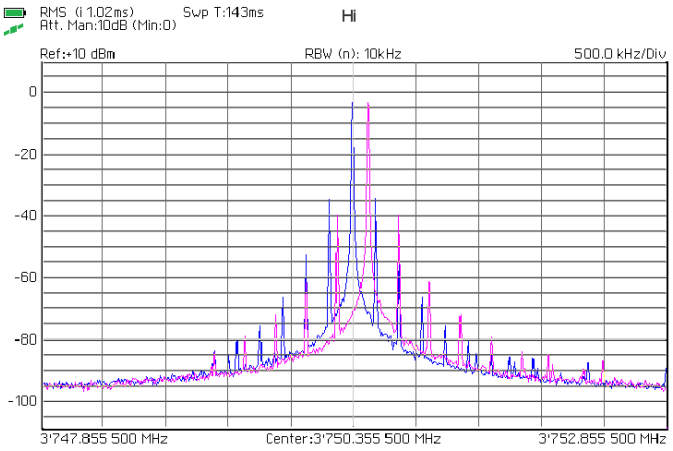

Figure 5. Locked PLL LMX9522 used in fractional mode with Numerator=3 (blue) and Numerator=4 (magenta), and Denominator=96, given PFD=5.89622 MHz.

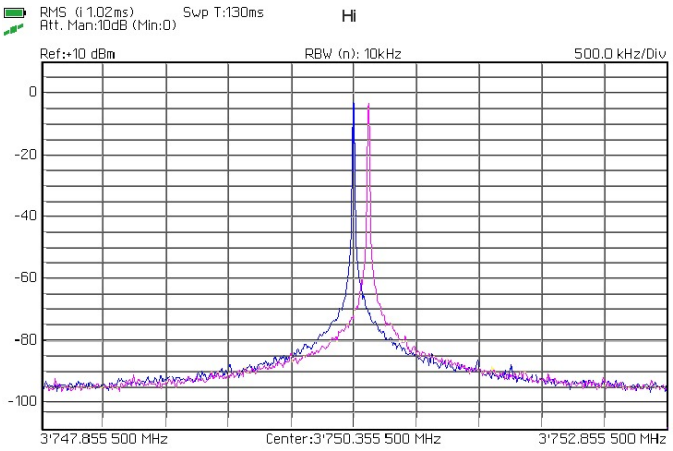

Figure 6. CA-controlled LMX9522; reference programmed to 3.7503685 GHz (blue) and 3.7504914 GHz (magenta).

tions of the ADG709 RF switch). The adjusting rate triggered by the CA is a direct consequence of the width value. Smaller widths imply higher rate (given constant leakage currents). As can be demonstrated theoretically [11], the adjusting speed can be tuned calibrating k_{in} and k_{out} coefficients.

The discussed implementation of the CA can be simplified. Instead of ten reactions as in Fig. 2, reactions can be cut down to two by letting the concentrations of species EU and ED reflect directly the positive and negative frequency error (which should be computed traditionally). This simplification, which drastically reduces the required computations, does not change the overall analysis and the experimental behaviour of the CA-controlled frequency synthesiser.

The implementation of the CA module (which included both an FPGA and a microcontroller) can be completely realised on FPGA solely, and eventually on ASIC. Previous works in the context of computer network traffic controllers [9] have described accurately an FPGA platform where any chemical reaction controller can be implemented. For example, if we consider the simplified reaction system just discussed, when expressing the reaction coefficient as single precision floating point and concentration as 16-bit integer, we can define a reaction coefficient k-ROM of 2x32 bit size, a concentration c-RAM of 3x16 bit size, and stoichiometric reactant α-RAM and stoichiometric product β-RAM of 2x1x1x1 bit size both, according to the guidelines given in [9].

The proposed CA-controlled frequency synthesiser relies on detecting the frequency difference between the output and the reference tones rather than the phase difference. This feature is not fundamental for the CA-based functioning, still frequency-detection rather than phase-detection helps preventing deadlock conditions. On the other hand, the CA-controlled frequency synthesiser, as proposed in this paper, does not allow phase locking.

V. Conclusion

In this paper, we propose a novel approach to frequency synthesis. This solution, which borrows principles from chemical kinetics, replaces the classic way of compensating the frequency error; compensation actions have all the same intensity but are scheduled with a rate that is proportional to the detected error. This brings benefits in terms of output spectral purity. We have implemented on hardware the Chemistry-inspired synthesiser and proved that it can improve the performance of an excellent on-the-market PLL.

References

[1] F. Gardner, "Charge-pump phase-lock loops", *IEEE Trans. on Communications*, vol. 28, no. 11, pp. 1849–1858, 1980.

[2] D. Biswas and T. K. Bhattacharyya, "Causes of PLL spurs and their modeling", *Analog Integr. Circuits Signal Process.*, vol. 100, no. 3, 2019.

[3] L. Liu, N.-J. Wu, J. Yang, J. Liu, and Z. Zhang, "Source-switched charge pump with reverse leakage compensation technique for spur reduction of wideband PLL", *Electronics Letters*, vol. 52, pp. 1211–1212, May 2016.

[4] X. Gao, E. A. M. Klumperink, G. Socci, M. Bohsali, and B. Nauta, "Spur reduction techniques for phase-locked loops exploiting a subsampling phase detector", *IEEE J. of Solid-State Circuits*, vol. 45, no. 9, pp. 1809–1821, 2010.

[5] H.-G. Ko, W. Bae, G.-S. Jeong, and D.-K. Jeong, "Reference spur reduction techniques for a phase-locked loop", *IEEE Access*, vol. 7, pp. 38 035–38 043, 2019.

[6] X. Liu and T. Chen, "Synchronization analysis for nonlinearly-coupled complex networks with an asymmetrical coupling matrix", *Physica A: Statistical Mechanics and its Applications*, vol. 387, no. 16–17, pp. 4429–4439, 2008.

[7] R. Staszewski *et al.*, "All-digital PLL and transmitter for mobile phones", *IEEE J. of Solid-State Circuits*, vol. 40, no. 12, pp. 2469–2482, 2005.

[8] S. M. Dartizio *et al.*, "A low-spur and low-jitter fractional-N digital PLL based on an inverse-constant-slope DTC and FCW subtractive dithering", *IEEE J. of Solid-State Circuits*, vol. 58, no. 12, pp. 3320–3337, 2023.

[9] M. Monti, M. Sifalakis, C. F. Tschudin, and M. Luise, "On hardware programmable network dynamics with a Chemistry-inspired abstraction", *IEEE/ACM Trans. on Networking*, vol. 25, no. 4, pp. 2054–2067, 2014.

[10] M. Monti, L. Sanguinetti, C. F. Tschudin, and M. Luise, "A Chemistry-inspired framework for achieving consensus in wireless sensor networks", in *IEEE Sensors J.*, vol. 14, Feb 2014, pp. 371–382.

[11] M. Monti, *Artificial physical Chemistry: Analysis and design of networking and communication systems*, Ph.D. Dissertation, University of Basel, Switzerland, 2014, Available: https://doi.org/10.5451/unibas-006318135.